Nonlinear strain effects in ion-implanted GaAs

B. M. Paine[a] and V. S. Speriosu[b]
Electrical Engineering 116-81, California Institute of Technology, Pasadena, California 91125

(Received 1 December 1986; accepted for publication 27 April 1987)

The nonlinear production of strain in (100) GaAs by room-temperature ion implantation has been studied. Ions of Ne, Si, and Te were used, with energies of 300, 300, and 500 keV, respectively. Doses ranged up to those required for amorphization. Strains were monitored by x-ray double-crystal diffractometry. Rocking curves were recorded about the (400) Bragg condition and detailed depth profiles of strain perpendicular to the sample surface, $\epsilon^{\perp}(x)$, found by fitting the rocking curves with a kinematic model. These were compared with calculated profiles of the density of energy deposited in nuclear interactions, $\rho_E(x)$. Rocking curves were also recorded about the (422) Bragg condition for selected samples, to monitor strain in the direction parallel with their surfaces. At low doses, $\epsilon^{\perp}(x)$ is a linear function of $\rho_E(x)$. At doses sufficient to create strains exceeding about 0.3%, strong nonlinearities are evident and strain profiles depart significantly from the $\rho_E(x)$ curves. For the Ne and Si implantations, the profiles tend to saturate at 0.4%–0.5% over a depth of ~4000 Å. At higher doses a narrow (~2000 Å), sharply peaked region develops, with strains up to 1.5%. At still higher doses this region becomes amorphous. The Te-implanted samples do not experience appreciable saturation; rather a sharply peaked profile develops, and grows with dose to amorphicity. Curves of $\epsilon^{\perp}$ vs ρ_E were extracted by comparison of $\epsilon^{\perp}(x)$ and $\rho_E(x)$ profiles. These demonstrated that for each ion species $\epsilon^{\perp}$ is a unique function of ρ_E at all depths. Although this function has the same general form for all three implantations, the curves differ from species to species. Above $\epsilon^{\perp} = 0.3\%$, $\epsilon^{\perp}$ increases sublinearly with ρ_E for all three implanted ions. For Ne and Si, $\epsilon^{\perp}$ becomes almost constant at 0.4%, beginning at $\rho_E \sim 0.15$ eV/Å^3. The strain $\epsilon^{\perp}$ starts increasing again with ρ_E at about 0.7 eV/Å^3 for Ne and 0.3 eV/Å^3 for Si, until the GaAs goes amorphous. The curve for Te shows only a slight inflection at $\epsilon^{\perp} \sim 0.3\%$, continuing to increase with ρ_E to amorphicity. Parallel strains in the Si-implanted samples were not more than 0.02% at all values of ρ_E.

INTRODUCTION

The structural changes that occur in GaAs as a result of keV ion implantation are still not well understood. Observations to date and relevant models have been reviewed recently by Sadana.[1] A parameter which is particularly sensitive to atomic displacements in crystals is strain. It can be measured as a function of depth with high accuracy by means of x-ray double-crystal diffractometry (DCD), in conjunction with iterative fitting of the resulting "rocking curves" with a theoretical model for the diffraction. In another paper,[2] we reported on a DCD study of low dose room-temperature implantations in (100) GaAs. It was found that at low temperatures $\epsilon^{\perp}$, the strain in the direction perpendicular to the sample surface, can be found from the expression

$$\epsilon^{\perp}(x) = K\phi F_D(x) = K\rho_E(x), \qquad (1)$$

where ϕ is the irradiation dose, $F_D(x)$ is the average energy per ion, deposited by nuclear collisions, per unit depth, at depth x, and K is a constant equal to $(5 \pm 1) \times 10^{-2}$ Å^3/eV. The quantity $\rho_E(x)$ is the average amount of energy deposited by collisions per unit volume at depth x. In this paper we report on strain measurement in (100) GaAs implanted at room temperature with higher doses, ranging up to those sufficient for amorphization.

Early DCD studies of implantation-induced strain in GaAs were concerned only with the maxima in the distribution of strain. It was found that the maximum perpendicular strain, $\epsilon^{\perp}_{max}$, does not vary linearly with dose at moderate doses,[3] and strain parallel to the surface of the sample (denoted $\epsilon^{\parallel}$) is negligible.[4] More recently[5] it was found that for 300-keV implantations of Si ions in GaAs, $\epsilon^{\perp}_{max}$ varies linearly with dose at low doses, but saturates above about 5×10^{13} ions/cm^2. Wie and co-workers[6,7] found that under implantation with 15-MeV Cl ions, perpendicular strain in (100) GaAs initially increased linearly with dose, but saturated at 0.4% at high doses, while parallel strain was always negligible.

PROCEDURE

Samples of (100) GaAs were prepared and implanted at room temperature, as described earlier.[2] Ions of Ne, Si, and Te were used to cover the range of masses that are normally used for electrical doping of GaAs. The energies were 500 keV for Te and 300 keV for the Ne and Si, giving roughly the same projected ranges for all three ions. For each ion species, about 12 different doses were implanted, ranging from the lowest sufficient to give easily perceptible strain (5–30×10^{11} ions/cm^2) up to those sufficient for amorphization

[a] Present address: Torrance Research Center, Hughes Aircraft Company, Torrance, CA 90509-2940.
[b] Present address: IBM Almaden Research Center, San Jose, CA 95120-6099.

 0021-8979/87/171704-06$02.40

(2×10^{13}–1×10^{15} ions/cm^2). Heat sinking compound was used and currents kept below 0.2 μA/cm^2, to minimize beam heating.

Analysis was conducted by Bragg case x-ray double-crystal diffraction (DCD) with Fe$K\alpha_1$ radiation and a (400) reflection in a (100) GaAs first crystal.[2] (400) rocking curves were recorded for all samples to monitor strain in the direction perpendicular to the surface, $\epsilon^{\perp}$. Since Laue back-diffraction measurements showed that the (100) axis was normal to the sample surface to within 0.5°, no asymmetry corrections were necessary. Note, by strain we mean change in the lattice parameter relative to that in the undisturbed bulk materials. (422) rocking curves were measured for some of these samples in order to monitor parallel strain. The {422} planes have a tilt relative to the {100} surface of $\psi = 35.3°$ and a Bragg angle, $\theta_B = 57.0°$. Measurements were made with the incident beam at an angle of $(\theta_B + \psi)$ from the sample surface, and the diffracted beam at $(\theta_B - \psi)$. About half the implantations were repeated; the resulting rocking curves always reproduced the original ones to within 5%. Several samples were also reanalyzed after storage for about six months. These rocking curves also reproduced the originals to within a few percent.

For each (400) rocking curve, an approximate measure of the maximum perpendicular strain $\epsilon^{\perp}_{\max}$ was obtained from the deviation of the lowest-angle oscillation of significant intensity from the substrate peak $\Delta\theta_0$, by the expression

$$\epsilon^{\perp}_{\max} = -\cot(\theta_B)\Delta\theta_0, \qquad (2)$$

where θ_B is the Bragg angle for unstrained GaAs. Profiles of strain as a function of depth were also deduced from most of the rocking curves by means of iterative fitting with a kinematic model for the diffraction.[8] This method also gives profiles of "damage," meaning the widths of the distributions (here assumed to be Gaussian) of the displacements of atoms from their mean positions. The calculation is performed for a perfectly collimated beam and perfectly planar crystal planes. The resulting rocking curve is then convolved with a Gaussian function, usually with standard deviation of about 0.002°, to account for slight divergence of the incident beam and lateral variations in the sample. Details are given in Ref. 2.

Complementary analyses were conducted on several samples by backscattering spectrometry (BSS) with channeling. The energy spectrum of channeled ions that are backscattered gives a direct qualitative measure of the profile of displaced atoms as a function of depth. While DCD is most sensitive to low levels of crystalline strain and damage, BSS is most applicable to highly damaged crystals or amorphous layers.[9] 1.5-MeV He ions were used, and backscattered particles detected at a scattering angle of 170°. Since in certain cases a MeV ion beam is known to change the strains in III-V materials (see e.g., Ref. 10), the BSS measurements were conducted only after the DCD measurements were complete.

RESULTS AND DISCUSSION

Departures from linearity immediately become apparent in the dependence of maximum perpendicular strain on implantation dose. Figure 1 shows such curves measured for the Si and Te implantations. Here data are plotted from the lowest dose implantation up to doses where the low angle structure in the rocking curves indicates a resumption of increasing strain with increasing dose. The uncertainties in these data are approximately the size of the plotted symbols, except where error bars are actually drawn. The dependence is linear at the lower doses, but drops to clearly sublinear behavior at higher doses. The departure from linearity occurs for $\epsilon^{\perp}_{\max}$ above about 0.3%. The solid lines in the figure are linear fits applied to the lower dose data. The curve for Ne, which lies very close to that for Si, was omitted for clarity.

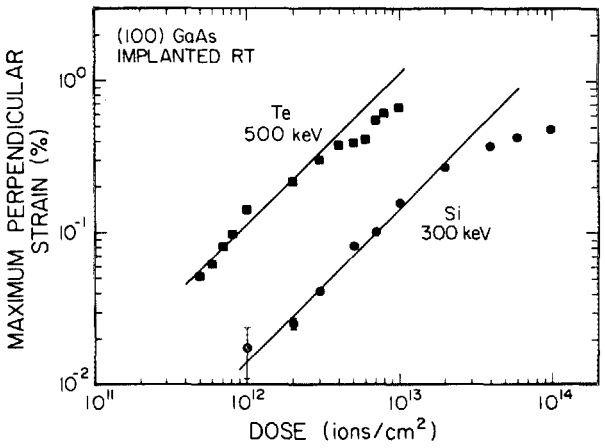

FIG. 1. Maximum perpendicular strain ($\epsilon^{\perp}_{\max}$) plotted as a function of dose for implantations of Si and Te into GaAs. Where error bars are not drawn, uncertainties are of the order of the size of the drawn symbols.

The onset of nonlinear dependence of $\epsilon^{\perp}$ on dose is accompanied by a change in the form of the rocking curves. Whereas at low doses the observed oscillations were all comparable in size,[2] at the higher doses of Fig. 1 the rocking curves show a single large peak at the greatest separation from the substrate peak, with many oscillations of mostly an order of magnitude lower intensity lying between the two. A typical example is shown as the dashed curve in Fig. 2. The

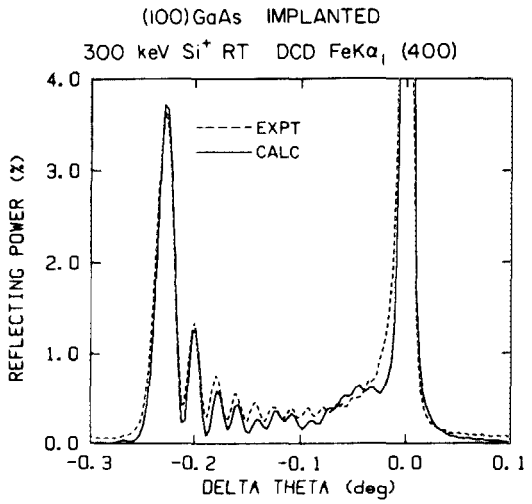

FIG. 2. Example of rocking curves for implantation dose in the nonlinear regime (here 6×10^{13} ions/cm^2).

large Bragg peak resulting from diffraction in undisturbed material is clear in the figure at $\Delta\theta = 0$. Structure is also visible at negative $\Delta\theta$ and arises from diffraction in material which is positively strained by the implantation. The solid curve in this figure is the fit, obtained by kinematic modeling with the input strain profile shown in Fig. 3 (upper curve). The quality of the fit in Fig. 2 is good—the largest two peaks near $\Delta\theta = -0.23°$ are well reproduced, and all of the observed small peaks appear in the calculated curve with only small discrepancies in position and amplitude. Removal of those discrepancies would require alterations of the strain profile of Fig. 3 of less than 5% of the maximum strain. Considering now the substrate signals, we note a small discrepancy on the low angle side. This may arise from the separate treatment of the strained layer and the substrate in this model.[8]

Figure 3 shows the profile of perpendicular strain for the fit of Fig. 2. For comparison, the profile for a dose of 2×10^{13} Si ions/cm^2 is also shown. The maximum in the latter is about 0.29%. It was reported earlier[2] that for doses in this vicinity the $\epsilon^{\perp}(x)$ curve is very similar to the distribution of energy deposited in atomic displacements, calculated in a Monte Carlo simulation. At 6×10^{13} Si ions/cm^2, the maximum of $\epsilon^{\perp}$ has obviously not increased by a factor of 3, and the profile has become less sharply peaked.

Similar saturation behavior was observed for the Ne implantations. Figure 4 shows a representative selection of the rocking curves recorded for the Ne implantations, together with the calculated fits and corresponding distributions of strain and damage. In part (a) the strain profile is close to the calculated distribution of energy deposited by atomic displacements. Its maximum is about 0.25%. For higher doses, the strains all increase. Those that were well below 0.3% increase linearly with the dose, while those that were higher rise less and less rapidly. The result is a flattening of the strain profile, as shown in part (b) for 2×10^{14} Ne ions/cm^2. This plateau becomes more and more prominent with higher doses until at around 5×10^{14} Ne ions/cm^2 the profiles change dramatically: a region about 3000 Å thick, at the depth where the plateau occurred at lower doses, rapidly develops a strain of about 0.8%, while at other depths the previously observed behavior continues [see Fig. 4(c)]. This sudden new element in the strain profile is clearly indicated in the rocking curves by the appearance of several more peaks, at values of $\Delta\theta$ below the prominent peaks corresponding to the plateau. Its thickness is well defined by the spacing of these peaks, while the existence of remnants of the plateau is indicated by the still-dominant structure at $\Delta\theta \sim -0.24°$. Fitting of the rocking curve in Fig. 4(c) was difficult because of the large number of peaks involved and the relatively steep variations of strain with depth. A better fit could have been obtained by using a larger number of steps to represent the strain curve in the steepest regions. But since the general shape, plus all of the peaks, are reproduced by the calculation, we believe that fitting with a large number of laminae would not yield a significantly different strain profile.

At still greater doses, the highly-strained region broadens and ceases to produce a signal in the rocking curve. This

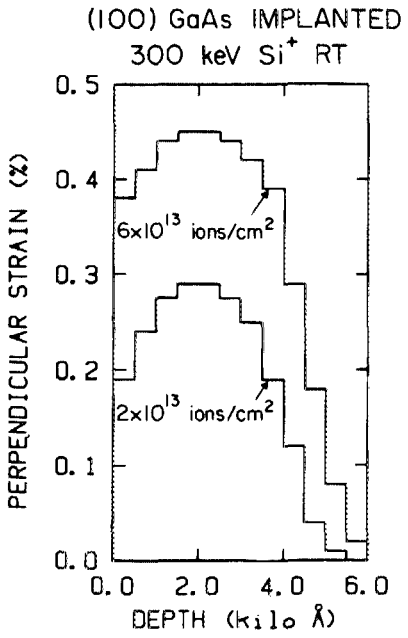

FIG. 3. Strain profile used for the fit of Fig. 2 (6×10^{13} ions/cm^2) compared with the profile measured in the linear regime (2×10^{13} ions/cm^2).

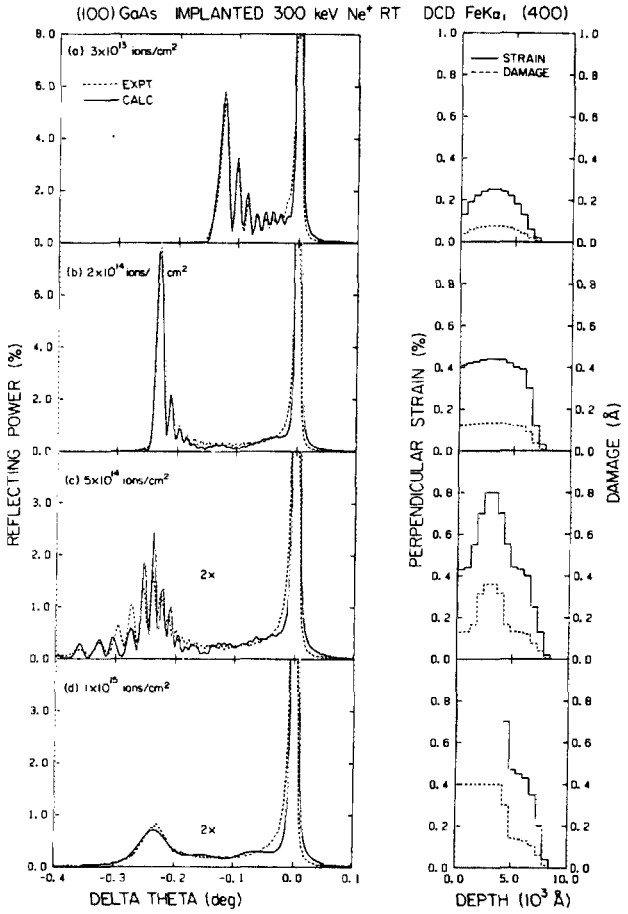

FIG. 4. Fitted rocking curves and the resulting strain and damage distributions for implantations with 300-keV Ne ions. This selection shows the onset of saturation (a) and (b), formation of the highly strained peak (c), and amorphization (d).

we interpret as full amorphization of this region. The remaining structure can be fitted reasonably well by assuming continuity of the development at lower doses: a ~3000-Å-thick transition region remains, with a variation from high strain adjacent to the amorphous region to zero strain beyond the range of the ions. Since the strain is not measurable by this method in amorphous material, the strain profile is not drawn in this region. The value of the damage parameter here of 0.4 Å is the minimum value needed to calculate essentially zero reflection power, i.e., the material is amorphous. We note that the rocking curve for this sample no longer has the rapid oscillations exhibited at lower doses. Indeed, for the fit shown in Fig. 4(d), the calculated curve was convolved with a Gaussian function of standard deviation 0.02°, as opposed to ~0.002° for all other curves. This indicates that the lateral coherence (or uniformity) of the layer has deteriorated. The observed broadening corresponds to strain variations of up to ~0.03%, or local deviations in orientation of up to ±0.02°.

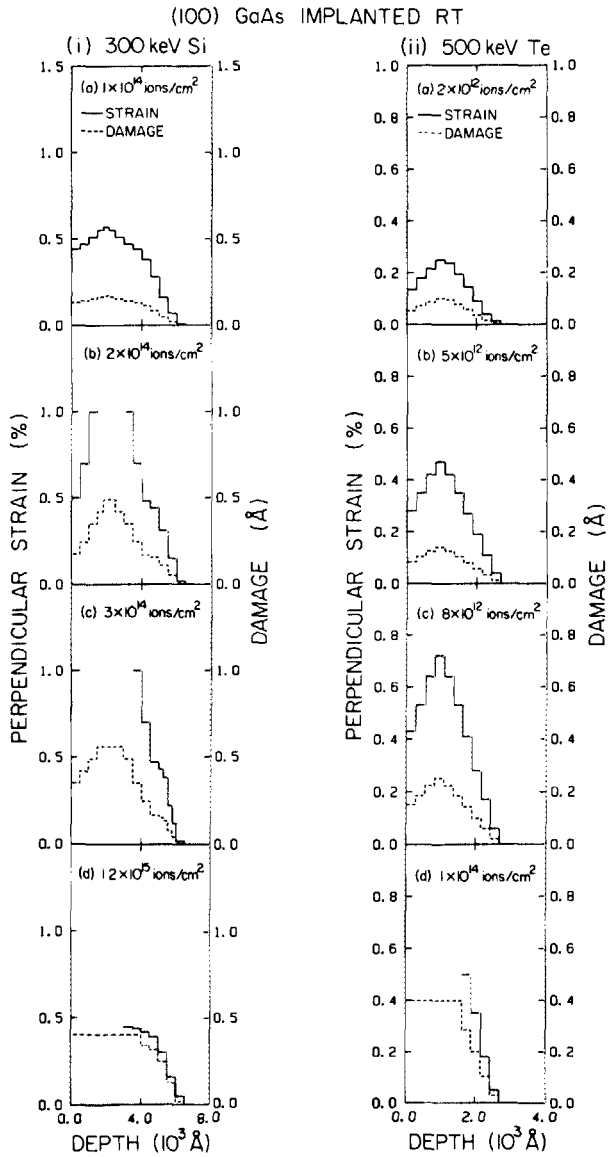

FIG. 5. Representative strain and damage distributions for various implantation doses of (i) 300-keV Si ions and (ii) 500-keV Te ions.

The rocking curves recorded for the Si implantation showed the same evolution as for Ne. A representative series of strain and damage profiles deduced by fitting are shown in Fig. 5(i). A selection of the calculated profiles for Te is shown in Fig. 5(ii). For the latter ions, the strains ceased to increase linearly with dose above about 0.3%, but essentially no saturation was observed, even though the implantation doses were incremented in steps of 1.0×10^{12} ions/cm^2 in the regime where it was expected by analogy with the Ne and Si results. Instead, a relatively broader high-strain region developed before going amorphous.

Backscattering measurements with channeling were made for some of the Si-implanted samples. The spectra are shown in Fig. 6 for doses for 1.5, 3, and 12×10^{14} ions/cm^2. The strain profiles for the latter two are shown in parts (c) and (d) of Fig. 5(i). The curve for 3×10^{14} ions/cm^2 shows high dechanneling, beginning at a depth of 1700 Å. This corresponds to the depth at which the strain reaches ~1.5%. The channeled spectrum for a dose of 12×10^{14} ions/cm^2 reaches the random level over a depth of 3000 Å, which is consistent with the conclusion that the highly strained region had become amorphous.

The strain profiles in the nonlinear regime were compared in a point-by-point fashion with those in the linear regime to find how perpendicular strain depends on density of energy deposited in each implantation. The procedure, which was applied to the series of $\epsilon^{\perp}(x)$ profiles obtained for each ion species, is shown schematically in Fig. 7. First the strain profile with $\epsilon^{\perp}_{max}$ just below 0.3% was adopted as the "low-dose" profile. This was the curve in the linear regime

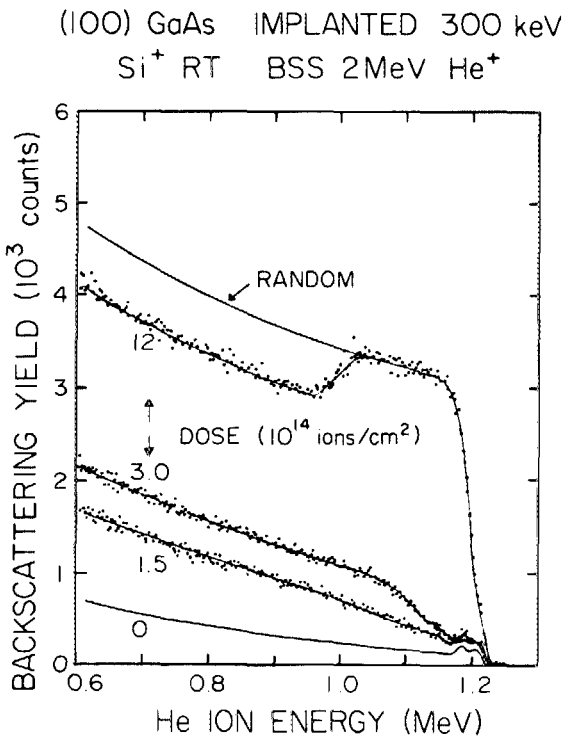

FIG. 6. Channeled backscattering spectra for samples implanted with 300-keV Si ions. Spectra for a (100) axially aligned piece of unimplanted GaAs and a randomly oriented piece are also shown for reference. 1-keV interval on the energy scale corresponds to a depth of 17.2 Å.

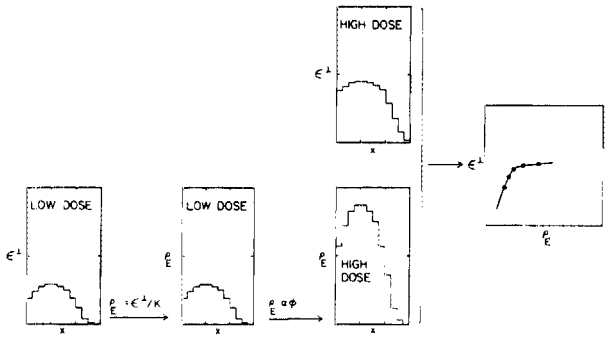

FIG. 7. Schematic diagram of the procedure used to find $\epsilon^{\perp}$ as a function of ρ_E for a "high dose" implantation. First $\rho_E(x)$ is taken to be proportional to a "low dose" $\epsilon^{\perp}(x)$ curve; then $\rho_E(x)$ is scaled up according to dose. Pairs of points are then read from the $\rho_E(x)$ and $\epsilon^{\perp}(x)$ curves at the same depths.

derived from the rocking curve with the maximum amount of structure. These corresponded to doses of 3×10^{13}, 2×10^{13}, and 2×10^{12} ions/cm^2 for Ne, Si, and Te, respectively. Since a very good fit had been obtained for each of the rocking curves, these strain profiles were the most accurate measured in the linear regime. Now, using the linear relation found earlier[2] between $\epsilon^{\perp}(x)$ and average density of energy deposited in atomic displacements ρ_E, we converted the $\epsilon^{\perp}(x)$ curve to $\rho_E(x)$. This linear relation between $\epsilon^{\perp}(x)$ and $\rho_E(x)$ profiles was specifically found to be correct for low dose Si^+ implantations in our previous work.[2] Also strong evidence for its validity was found for implantation with a wide range of ions. An alternative approach would have been to calculate $\rho_E(x)$ with a theoretical simulation of the collision cascades caused by the incident ions. However, it was felt that measurement of $\rho_E(x)$, in the form of a strain profile, was probably more accurate. Once the $\rho_E(x)$ curve had been found for the "low dose" implantation, it was scaled with dose to give the appropriate curve for each higher-dose implantation. Now for each pair of plots [$\epsilon^{\perp}(x)$ and $\rho_E(x)$ for a given dose], values of $\epsilon^{\perp}$ and ρ_E were read off at each depth interval (i.e., at each lamina). The thicknesses of the laminas in all of the $\epsilon^{\perp}(x)$ curves had been kept the same to facilitate this. Thus, for each dose a series of $\epsilon^{\perp}$ vs ρ_E points was obtained. These are plotted with different symbols for each dose in Fig. 8.

Figure 8 shows the same linear dependence of $\epsilon^{\perp}$ on ρ_E at low values of ρ_E for all three implantations. This is true by definition for the dose used to deduce $\rho_E(x)$, but was confirmed by the low strain data for all other implantations. In fact, many of the low-strain (but higher-dose) points were omitted from Fig. 8 because they would have been drawn directly over other symbols. This behavior is consistent with the universal relationship between $\epsilon^{\perp}$ and ρ_E reported earlier.[2]

For higher-energy densities the Ne and Si data show a definite saturation at a strain of about 0.4% before increasing again, while the Te data show only a slight inflection at about 0.3%. For the Ne implantation, the saturation extends from $\rho_E = 0.1$–0.6 eV/Å^3. Points at the same value of ρ_E, arising from different doses, were necessarily measured at different depths in the GaAs. Therefore, the fact that all data

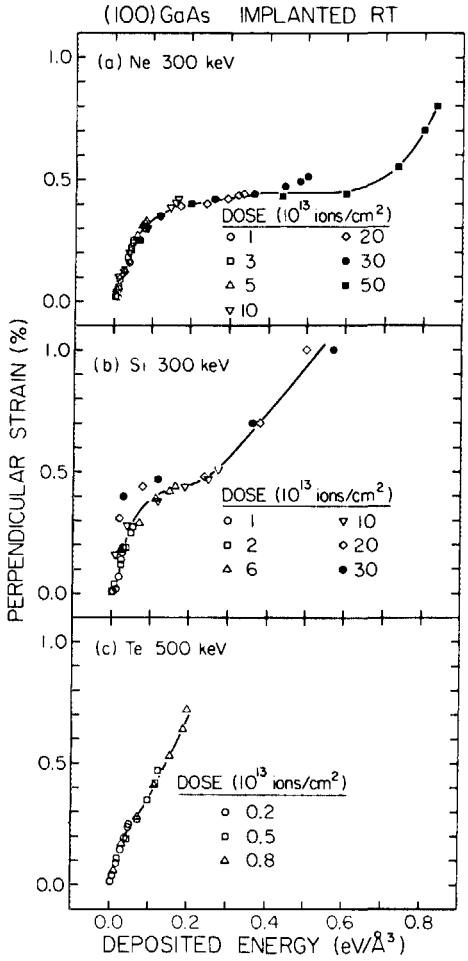

FIG. 8. Plots of perpendicular strain $\epsilon^{\perp}$ as a function of density of energy deposited by nuclear interactions, ρ_E. Each series of points for a particular ion species and dose was deduced from a single rocking curve, together with the $\rho_E(x)$ distribution. The method is shown schematically in Fig. 7.

points lie close to the same curve for each ion species indicates that $\epsilon^{\perp}$ is a unique function of ρ_E, independent of depth. However, Fig. 8 demonstrates that this function is not only nonlinear, but varies from one ion species to another, with the saturation apparently diminishing with increase in the mass of the implanted ions.

Finally, asymmetric (422) rocking curves were recorded for two samples implantated with different doses of Si. These are shown as dashed lines in Fig. 9, with fits plotted as solid lines. This particular diffraction condition was chosen for its high sensitivity to parallel strain. As an example, a change in the parallel strain of 0.02% would shift the calculated peaks in Fig. 9 by 0.01°, making a clearly perceptible change in the quality of the fits. The doses were 6×10^{13} ions/cm^2, which was shown to generate saturation of perpendicular strain over a large portion of the implanted region (see Fig. 3), and 2×10^{14} ions/cm^2, at which dose the highly strained region has developed [see Fig. 5(i)(b)]. The fits were calculated assuming precisely the perpendicular strain distributions found earlier by fitting the (400) rocking curves, together with parallel strains, assumed to be constant throughout the implanted regions. The Gaussian broadening functions had widths of 8 and 9×10^{-3}°, respectively. These were larger than those used for the (400) diffractions

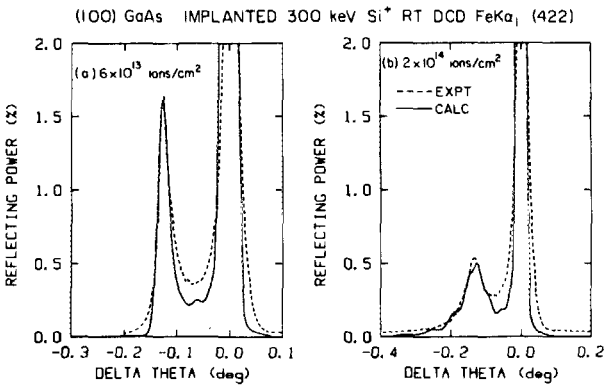

FIG. 9. *Asymmetric (422) rocking curves for two of the Si implantations.* The fits were obtained with exactly the distributions of perpendicular strain deduced from the (400) rocking curves, shown in Figs. 3 and 5(i)(b), together with a parallel strain, assumed constant throughout the strained region. The values were -0.01% for (a) and -0.02% for (b).

($\sim 3\times 10^{-3}$°) because the finite energy width of the beam broadens the rocking curve structure in this dispersive configuration. The quality of the fits is satisfactory. The discrepancies at $\Delta\theta$ lying between the main peaks arise from small errors in the profile which were also evident in Fig. 2. The parallel strains deduced from these fits were $(-0.01\pm 0.01)\%$ for the dose of 6×10^{13} ions/cm^2 and $(-0.02\pm 0.01)\%$ for 2×10^{14} ions/cm^2.

Since little is known of the effect of other parameters, e.g., temperature, on these phenomena, one can only speculate on the responsible physical mechanisms. The saturation cannot be explained simply as relaxation in the direction parallel with the sample surface because no parallel strain was observed. Compressive stress probably arises from interstitial atoms, as well as other defects. The concentration of defects may increase linearly with irradiation dose at low doses where the probability of interaction of defects is low. At higher doses, recombination of defects may lead to the observed saturation behavior. Wie, Tombrello, and Vreeland[7] proposed such a model assuming strain depends on the concentration of antisite defects. If this model is correct, the high strains at higher doses may occur because the heavy damage in the lattice curtails the defect migration. Alternatively, the saturation may result from aggregation of defects at points where they no longer contribute to strain, e.g., amorphous regions.

Several important questions should be addressed in future work. The role of defect migration can be investigated by repeating the measurements at different implantation temperatures. Preliminary liquid-nitrogen temperature and room-temperature measurements with phosphorus implantations showed saturation over a smaller range of doses for the lower temperature. This supports the hypothesis that migration of defects contributes to the saturation phenomenon. Further measurements should also be conducted with different ion species to see whether the threshold for formation of the highly strained peak depends simply on the ion mass, as suggested by our results, or whether other correlations are present. Another important question is whether the saturation behavior is unique to III-V semiconductors. It has been observed in GaP (Ref. 11) but not in Si (Ref. 5), Ge (Ref. 5), or magnetic garnet.[12]

ACKNOWLEDGMENTS

N. N. Hurvitz assisted with some of the rocking curve measurements. This work was begun with financial support from the Defence Advanced Research Projects Agency (MDA 903-82-C-0348). It was completed with support from the Semiconductor Research Corporation (85-04-059).

[1]D. K. Sadana, Nucl. Instrum. Methods Phys. Res. B **7/8**, 375 (1985).
[2]B. M. Paine, N. N. Hurvitz, and V. S. Speriosu, J. Appl. Phys. **61**, 1335 (1987).
[3]G. F. Kalugina, F. N. Komaleeva, V. N. Mordkovich, I. M. Sukhodreva, and E. M. Temper, Sov. Phys. Semicond. **16**, 230 (1982).
[4]M. V. Prilepskii, I. M. Sukhodreva, and L. D. Cheryukanova, Sov. Phys. Tech. Phys. **27**, 384 (1982).
[5]V. S. Speriosu, B. M. Paine, M.-A. Nicolet, and H. L. Glass, Appl. Phys. Lett. **40**, 604 (1982).
[6]C. R. Wie, T. Vreeland, Jr., and T. A. Tombrello, Mater. Res. Soc. Symp. Proc. **35**, 305 (1985).
[7]C. R. Wie, T. A. Tombrello, and T. Vreeland, Jr., Phys. Rev. B **33**, 4083 (1986).
[8]V. S. Speriosu, J. Appl. Phys. **52**, 6094 (1981).
[9]B. M. Paine, V. S. Speriosu, L. S. Wielunski, H. L. Glass, and M.-A. Nicolet, Nucl. Instrum. Methods **191**, 80 (1981).
[10]C. K. Pan, D. C. Zheng, T. G. Finstad, W. K. Chu, V. S. Speriosu, M.-A. Nicolet, and J. H. Barrett, Phys. Rev. B **31**, 1270 (1985).
[11]C. R. Wie, T. Vreeland, Jr., and T. A. Tombrello, Nucl. Instrum. Methods B **44**, 44 (1986).
[12]B. E. MacNeal and V. S. Speriosu, J. Appl. Phys. **52**, 3935 (1981).